Journal of Structural Geology, Vol. 10, No. 7, pp. 765 to 770, 1988
Printed in Great Britain

0191-8141/88 $03.00 + 0.00

Brevia

SHORT NOTE

Seven types of subgrain boundaries in octachloropropane

W. D. MEANS and J. H. REE

Department of Geological Sciences, State University of New York at Albany, Albany NY 12222, U.S.A.

(*Received* 27 *July* 1987; *accepted in revised form* 29 *July* 1988)

Abstract—Subgrain boundaries in thin sheets of octachloropropane deformed at 0.7–0.8 T_M on the stage of a microscope are seen to appear in the material in seven different ways. Type I boundaries show the classical evolution by polygonization of bent crystals. Type II are essentially kink boundaries, which migrate sideways during deformation to reach their present positions in the crystals. Type III develop at the sites of former grain boundaries, by reduction of misorientation of adjacent grains. Type IV and V originate by impingement of migrating grain boundaries or subgrain boundaries, respectively. Type VI propagate in their own planes behind migrating grain boundaries to which they are attached. Type VII develop statically from optically strain-free grains by a process probably otherwise similar to the Type I process. Two thirds of the boundaries are Types I or II. In view of the variety of subgrain boundary histories in OCP, interpretation of similar features in minerals ought to be undertaken cautiously. Criteria are needed for telling the different types of subgrain boundaries apart in situations where only a final view of the structure is available, as in optical and electron micrographs of rocks.

INTRODUCTION

ONE OF the insights gained from recent direct observation of microstructural evolution in deforming polycrystals (see Urai 1987, Burg *et al.* 1986 and references therein for techniques) is that optical microstructure may not be very process-definitive. That is to say, a single optical microstructure may originate in more than one way, and thus not be a reliable 'structural signature' for any particular process. Independently, the same lesson is emerging from comparisons of optical and electron-optical micrographs (e.g. Tullis & Yund 1977, 1987). One optical microstructure may correspond to more than one electron-optical microstructure. We illustrate this inconvenient but important property of optical microstructure here using subgrain boundaries as an example. We show that subgrain boundaries having at least seven different origins can all look about the same in thin section views. Six of the seven types were found in a single deformed sample of octachloropropane (C_3Cl_8) (hereafter called OCP). OCP has been used in several previous microstructural studies by metallurgists and geologists (Beck 1949, McCrone 1949, Means 1983, Dong 1985, Jessell 1986, ter Haar *et al.* unpublished abstract, EUG IV Conference 1987). It is a soft, ductile, uniaxial positive, hexagonal material with a striking ability to develop the microstructures that are familiar from thin sections of naturally and experimentally deformed minerals, especially quartz.

EXPERIMENTAL DETAILS

Samples were prepared for deformation by pressing a mixture of OCP and 1000-grit silicon carbide particles between partially frosted glass slides at room temperature. The glass slides serve at once to contain the sample and to impose an approximate simple shear deformation upon it, in the manner explained by Means & Xia (1981). The silicon carbide particles allow the deformation progress to be followed, and assist in recognition of migration of grain boundaries and subgrain boundaries. Deformation of the sample described here was carried out at 65 ± 5°C (about 80% of the absolute melting point of OCP), at a strain rate of 3.1×10^{-5} s^{-1}, using a new, stage-mounted press designed by J. Urai (State University of Utrecht).

Figure 1 shows three maps of the sample (a) at the beginning of the deformation, (b) immediately following the deformation and (c) after a period of static adjustment at the deformation temperature, with the motor off but not backed-up. The thickness of the sample was 50 μm throughout the experiment, or about 25% of the diameter of the larger grains in the starting material. A bulk shear strain γ of about 1.4 was imposed.

The main microstructural effects of the deformation (cf. Figs. 1a & b) were the introduction of an oblique, grain-shape foliation that leans in the direction of shear and intersects it at 25–45°, some multiplication of subgrain boundaries and an 80% increase in average grain size. Photographs taken about every half-hour between the stages shown in Figs. 1 (a) and (b) show extensive dynamic recrystallization by grain boundary migration (as described by Means 1983, Jessell 1986). The microstructural effects of the period of static adjustment were limited further migration of grain boundaries eliminating some smaller grains, and local changes in subgrain geometry. The period with the motor off was a period of greatly reduced strain rate, but it was not entirely static, as comparison of the marker configuration in Figs. 1(b)

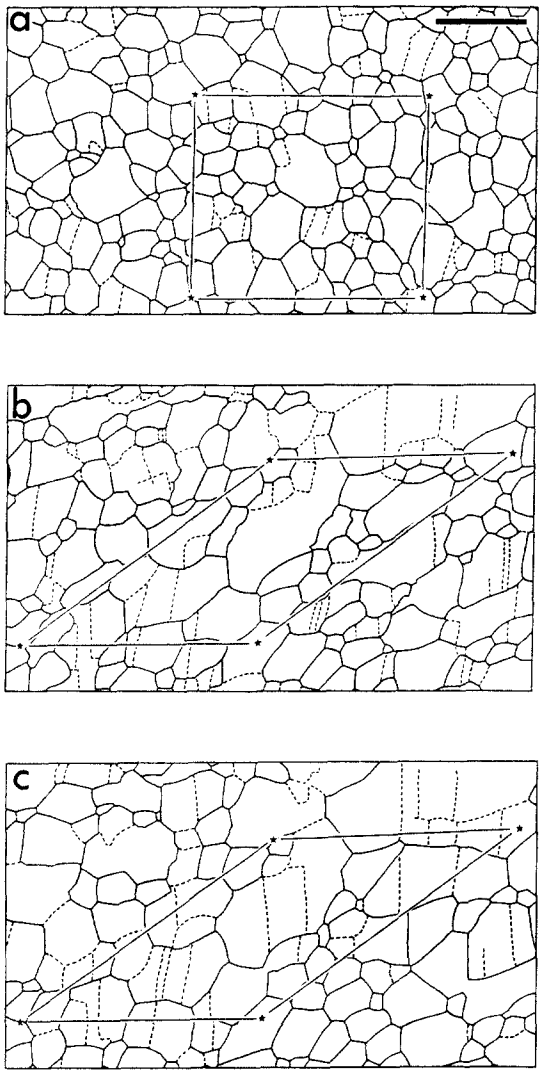

Fig. 1. Maps of octachloropropane sample TO-91, showing grain boundaries (heavy solid lines), subgrain boundaries (dashed lines) and the positions of four marker particles (stars) which show the bulk deformation geometry. The indicated deformation departs slightly from a simple shear in that there is a 4% extension in the shearing direction and an 8% flattening normal to it, with a consequent 4% reduction in area. (a) Microstructure immediately before deformation. Scale bar 300 μm. (b) Microstructure 12.25 hr later, immediately after deformation, when a shear strain (γ) of about 1.4 has accumulated on planes initially parallel to the edges of the marker box in (a). (c) Microstructure after 15 hr of approximately static adjustment at the deformation temperature. The photomicrographs of Figs. 3 and 4 correspond to γ values between those of (a) and (b), or times (t) between (b) and (c) as indicated in the figure captions.

and (c) will show. An additional shear strain of about 3% accumulated during the nominally static interval, presumably by relaxation of elastic strains in the driving system.

TYPES OF SUBGRAIN BOUNDARIES

Features like subgrain boundaries can be classified structurally or genetically. Genetic classifications in turn are of three types—classification by *structural history*, classification by *driving forces/mechanisms* and classification by *extrinsic conditions* of deformation. The genetic classification used here is the easiest one to establish using the present technique—classification by observed structural history. For each type of subgrain boundary we show a distinct temporal development of the structure. This kind of classification is presumably a useful step toward understanding the other kinds of genetic classes that exist and, ultimately, toward establishing the measurable properties of naturally deformed rocks that correspond to genetic classes of interest.

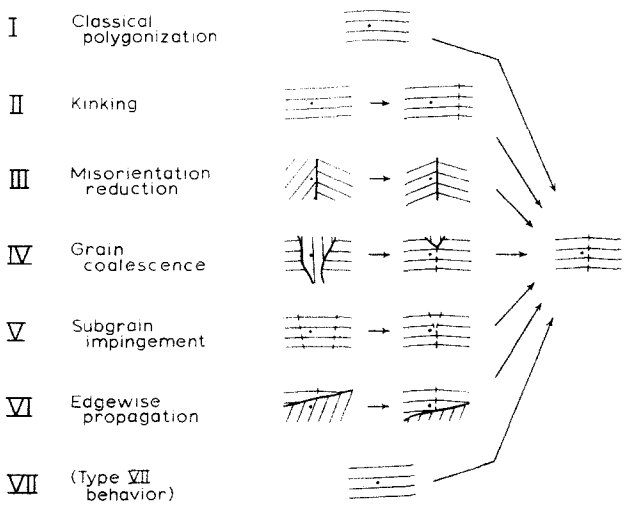

Fig. 2. Schematic representation of the seven types of subgrain boundary development. Heavy solid lines—grain boundaries. Dashed lines—subgrain boundaries. Light lines—traces of extinction direction at high angle to subgrain boundary (typically (0001) traces in OCP). Dot represents marker particle fixed in the material.

The subgrain boundaries described here are narrow (<10 μm wide) boundaries between parts of grains across which the extinction position differs abruptly by 1–8°. Subgrain boundaries of smaller misorientation than 1° may also have been present, but were not recognizable optically. In plain light (with one of the polarizing filters removed), the image of a subgrain boundary vanishes. Grain boundaries, on the other hand, typically separate regions with bigger differences in extinction directions, and have distinct images even in plain light. In plain light, grain boundaries in OCP are marked by distinct dark lines or by brightness discontinuities. Some boundaries in our sample are admittedly indeterminate as either grain boundaries or subgrain boundaries. This is not surprising in view of the origins discussed below. In terms of misorientation and internal structure, some boundaries probably *are* intermediate between 'good' grain boundaries and 'good' subgrain boundaries.

The seven types of subgrain boundaries are shown schematically in Fig. 2 and illustrated in Figs. 3 and 4.

Type I

Type I boundaries form by polygonization of regions of undulose extinction. They are presumably the classical type produced during static or dynamic recovery of crystals with bent lattices, by glide and climb of excess

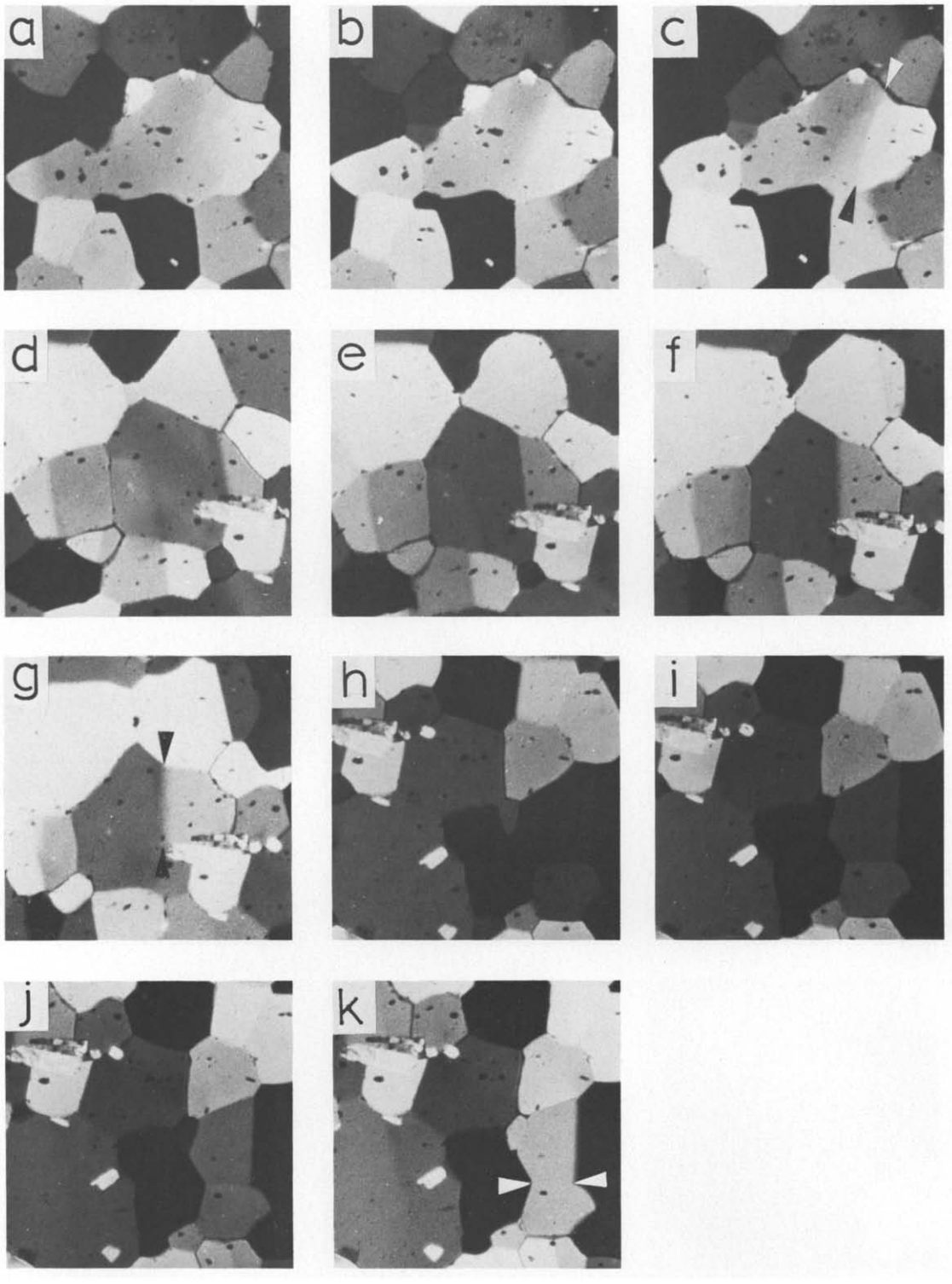

Fig. 3. Photomicrographs made during the deformation showing examples of Type I (a–c), Type II (d–g) and Type III (h–k) subgrain boundaries. Photo dimensions—425 μm per side. Most small black particles are silicon carbide markers. A few (which appear or disappear during a sequence) are small bubbles or voids. Medium-sized white fragments in (h–k) are bits of paper incorporated accidentally. Paired pointers in (c), (g) and (k) show subgrain boundaries that have behaved in Type I, II and III manner, respectively. Bulk shear strain (γ) values at start of each sequence and additional bulk shear strain ($\Delta\gamma$) accumulated during the sequence as follows: (a–c) $\gamma = 0.14$, $\Delta\gamma = 0.11$; (d–g) $\gamma = 0.00$, $\Delta\gamma = 0.33$; (h–k) $\gamma = 0.07$, $\Delta\gamma = 0.18$.

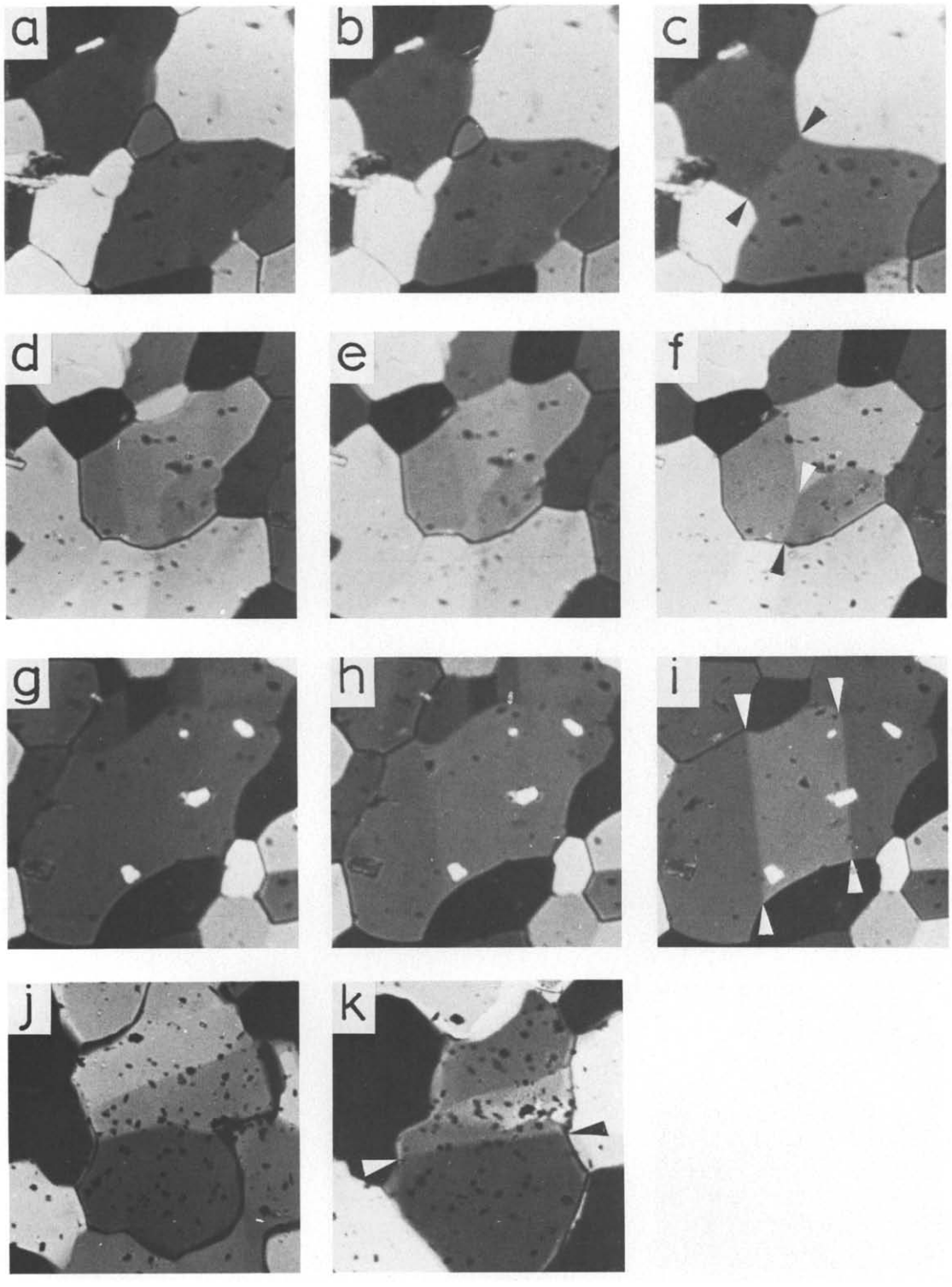

Fig. 4. Photomicrographs made during the static interval showing examples of Type IV (a–c), Type V (d–f), Type VII (g–i) and Type VI (j–k) subgrain boundaries. Scale, format, etc., as for Fig. 3. Times t after stage (b) (Fig. 1) and time interval (Δt) as follows. For (j–k), from experiment by Means (1983), ε and $\Delta\varepsilon$ give bulk shortening and bulk shortening increment. (a–c) t = 0.5 hr, Δt = 10 hr; (d–f) t = 0.5 hr, Δt = 14.5 hr; (g–i) t = 2.5 hr, Δt = 12.5 hr; (j–k) ε = 35%, $\Delta\varepsilon$ = 6%.

dislocations of one sign into low-energy, planar arrays. Type I boundaries may migrate laterally while they form, but this is not an essential feature. In the OCP example of Figs. 3 (a)–(c), there is migration, particularly of the lower part of the boundary. Type I boundary development does not require concurrent deformation of the grain, but this may occur.

Type II

Type II boundaries are essentially kink band boundaries, which migrate through a grain as deformation progresses to reach their current position. They require concurrent deformation for their arrival at a given position in a grain. The exceptional case of no migration for a Type II boundary is the case where the kinking produces perfectly symmetrical chevron folds in the active slip plane. Even here, concurrent deformation is essential, however, so Type II is not expected in a static environment. Type II subgrain boundaries form by 'glide polygonization' (Livingston 1960). Their migration under load is familiar to metallurgists (e.g. Exell & Warrington 1972). They are at once subgrain boundaries and a kind of deformation band boundary. The OCP example of Figs 3 (d)–(g) exemplifies migration behavior close to that of the idealized kink bands of Paterson & Weiss (1966). There is little syn-migration straining on either side of the subgrain boundary, but noticeable translation of the subgrain to the right of the boundary upwards, relative to the subgrain to the left of the boundary (use tracings of the marker particles to confirm this). The boundary migrates sidewise to accommodate the translation jump across it, as explained by Means & Jessell (1986).

Type III

Type III boundaries are subgrain boundaries that have evolved, more or less *in situ* (without migration), by reduction of the difference in lattice orientation between neighboring grains. They are 'ghost' grain boundaries. We surmise that Type III behavior requires concurrent deformation and that, in the simplest cases, it may be something like unkinking. In more general cases, where the dominant slip plane intersects the grain boundary in two very different orientations (from the two sides of the boundary), it is not clear how or whether the process operates. In the example of Figs. 3 (h)–(k) there are not enough markers in the grains to show what deformation is occurring within them. We know of no previous description of Type III behavior but imagine it has been observed before. It is to be expected only in deforming materials.

Type IV

Type IV boundaries form by coalescence of two grains with similar lattice orientations which were not initially in contact with each other, but which become neighbors by grain boundary migration and consumption of intervening grains. The OCP example in Figs. 4 (a)–(c) shows consumption of two intervening grains. Another example of Type IV behavior can be seen in the lower right-hand part of Figs. 3 (d)–(g), where a coalescence boundary forms by consumption of a small, dark-grey grain between two, lighter-grey, grains. Type IV behavior can occur whenever grain boundary migration can occur (i.e. in static or dynamic environments). A dynamic example has been illustrated by Urai *et al.* (1986, p. 185), and the static case has been discussed by Nielsen (1966). Type IV behavior is one way of increasing grain size during dynamic recrystallization.

Type V

Type V boundaries are similar in principle to Type IV but they form by impingement of migrating subgrain boundaries instead of grain boundaries. This process is known in statically recovered metals (Li 1966, p. 86) and can also occur in deforming materials (i.e. by impingement of two Type II boundaries). Our OCP example in Figs. 4 (d)–(f), shows a Y junction (where three subgrain boundaries meet) the stem of which formed by subgrain boundary impingement during the nominally static interval.

Type VI

Type VI boundaries are portions of boundaries that have grown or propagated in their own plane in order to remain connected to outward-migrating grain boundaries (grain boundaries migrating away from grain interiors). They are believed to develop as a simple consequence of the outward growth of the two adjoining subgrains. A static example was described by Means & Dong (1982), who referred to the process as 'edgewise propagation' of subgrain boundaries. An example in deforming OCP is shown in Figs. 4 (j)–(k). Note that only the outer extremities of the boundary in Fig. 4 (k) are clearly of Type VI origin. Note, too, that in this case the excess length of the boundary in Fig. 4 (k) over that in Fig. 4 (j) cannot be explained by plastic extension of the crystal in the E–W direction. This example is from a pure shear experiment (Means 1983) in which the material was being shortened in the E–W direction, not lengthened. Type VI behavior may involve some migration of the subgrain boundary as well as its edgewise extension. This is the case in Figs. 4 (j)–(k) and in the example of Means & Dong (1982).

Type VII

Type VII boundaries develop in optically 'strain-free' grains (grains with uniform interference color and intensity and uniform extinction), without benefit of any essential subgrain boundary migration process, and without large concurrent deformation (such as in Type II behavior). Figures 4 (g)–(i) shows an example. Type VII boundaries are probably similar in origin to Type I boundaries, except that they arise from regions of crystal

containing high densities of dislocations of *both* signs, so that the lattice is not bent on a scale that is optically recognizable. Type VII boundaries are accordingly expected to form chevron fold sets within individual grains (antiform–synform–antiform, etc.), while Type I boundaries should form repeated fold sets (antiform–antiform–antiform, etc.) over any part of the host grain with a uniform sense of lattice bending.

A survey of all the prominent subgrain boundaries in the sample showed that about two thirds were either Type I (26%) or Type II (41%), with Type III the other relatively common type (11%). Types IV, V, VI and VII, respectively, made up 3, 6, 5 and 8% of the total population of 62 subgrain boundaries surveyed.

DISCUSSION

The multiple origins of subgrain boundaries in OCP may or may not apply to subgrain boundaries seen in thin sections of naturally deformed minerals. They should be kept in mind however when interpreting natural examples. For example, the presence of subgrains in recrystallized grains is commonly taken as evidence of dynamic rather than static recrystallization. This may not be the correct interpretation if the subgrains are defined by boundaries of Types IV or VI.

Three approaches are available to improve understanding of how subgrain boundaries have developed in particular deformed rocks. There is the hope that by using TEM microstructure along with optical microstructure, some criteria for recognizing different kinds of subgrain boundaries will emerge. There is the possibility that measurements of lattice misorientations will help distinguish different types of subgrain boundaries. Finally, there is the certainty that the best interpretation of subgrain boundaries will emerge if they are considered together with other coeval microstructural features that are sensitive to the processes by which they have developed (like grain boundary configurations and grain-size distributions).

A final point is that subgrain boundaries can have complex histories. For example, it may be common in deforming materials for subgrain boundaries to initially develop as Type I boundaries and then to migrate in Type II fashion. We found many examples of this in the sample described above. Or during Type II migration, a boundary may incorporate slower- or reverse-moving boundaries, so that, instantaneously, it is Type V. The classification of Fig. 2 is a classification according to the most *recent history of a boundary*, not necessarily its entire history.

Acknowledgments—We thank J. Tullis and R. Knipe for helpful reviews, and B. Hobbs, M. Etheridge and R. Knipe for independently suggesting to us the interpretation of Type VII boundaries given above. Supported by U.S. National Science Foundation Grant EAR 8506810.

REFERENCES

Beck, P. A. 1949. Comments on grain growth in octachloropropane. *J. appl. Phys.* **20**, 231.

Burg, J. P., Wilson, C. J. L. & Mitchell, J. C. 1986. Dynamic recrystallization and fabric development during the simple shear deformation of ice. *J. Struct. Geol.* **8**, 857–870.

Dong, H. 1985. A possible formational process of mylonite. *Acta geol. Sinica* **4**, 286–292.

Exell, S. F. & Warrington, D. H. 1972. Sub-grain boundary migration in aluminum. *Phil. Mag.* **26**, 1121–1136.

Jessell, M. W. 1986. Grain boundary migration and fabric development in experimentally deformed octachloropropane. *J. Struct. Geol.* **8**, 527–542.

Li, J. C. M. 1966. Recovery processes in metals. In: *Recrystallization, Grain Growth and Textures* (edited by Margolin, H.), 1965 Seminar. American Society for Metals, 45–97.

Livingston, J. D. 1960. Etch pits at dislocations in copper. *J. appl. Phys.* **31**, 1071–1076.

McCrone, W. C. 1949. Boundary migration and grain growth. *Disc. Faraday Soc.* **5**, 158–166.

Means, W. D. 1983. Microstructure and micromotion in recrystallization flow of octachloropropane: a first look. *Geol. Rdsch.* **72**, 511–528.

Means, W. D. & Dong, H. 1982. Some unexpected effects of recrystallization on the microstructures of material deformed at high temperature. *Mitt. geol. inst. ETH, Neue Folge* **239a**, 205–207.

Means, W. D. & Jessell, M. W. 1986. Accommodation migration of grain boundaries. *Tectonophysics* **127**, 67–86.

Means, W. D. & Xia, Z. G. 1981. Deformation of crystalline materials in thin section. *Geology* **9**, 538–543.

Nielsen, J. P. 1966. The grain coalescence theory. In: *Recrystallization, Grain Growth and Textures* (edited by Margolin, H.), 1965 Seminar. American Society for Metals, 141–164.

Paterson, M. S. & Weiss, L. E. 1966. Experimental deformation and folding in phyllite. *Bull. geol. Soc. Am.* **77**, 795–812.

Tullis, J. & Yund, R. A. 1977. Experimental deformation of dry Westerly granite. *J. geophys. Res.* **82**, 5707–5718.

Tullis, J. & Yund, R. A. 1987. Transition from cataclastic flow to dislocation creep of feldspar: mechanisms and microstructures. *Geology* **15**, 607–609.

Urai, J. L. 1987. Development of microstructure during deformation of carnallite and bischofite in transmitted light. *Tectonophysics* **135**, 251–263.

Urai, J. L., Means, W. D. & Lister, G. S. 1986. Dynamic recrystallization of minerals. In: *Mineral and Rock Deformation: Laboratory Studies—The Paterson Volume* (edited by Heard, H. C. & Hobbs, B. E.). *Am. Geophys. Un. Geophys. Monogr.* **36**, 161–199.